ARTICLE

Grafting Poly(methyl methacrylate) onto Polyimide Nanofibers via "Click" Reaction

Zhenjun Chang, Yuan Xu, Xin Zhao, Qinghua Zhang, and Dajun Chen*

State Key Laboratory for Modification of Chemical Fibers and Polymer Materials, College of Materials Science and Engineering, Donghua University, Shanghai 201620, P. R. China

ABSTRACT Surface modification of azide-decorated polyimide (PI) nanofibers with well-defined alkyne-terminated poly(methyl methacrylate) (PMMA) was accomplished via the combination of atom transfer radical polymerization (ATRP) and "click" chemistry. In this work, PI nanofibers were prepared via electrospun polyamic acid (PAA), followed by thermal imidization. Grafting of PMMA onto PI nanofibers was accomplished in three steps: (1) choloromethylation and azidization of PI nanofibers; (2) preparation of alkyne-terminated PMMA by ATRP of methyl methacrylate in toluene using propargyl 2-bromopropionate as initiator; (3) click coupling between the azidized PI nanofibers and the alkyne-terminated PMMA under the catalysis of Cu(I)Br/N,N,*N*′,*N*″-pentamethyldiethylenetriamine (PMDETA). Gel permeation chromatography (GPC), ^{1}H NMR, and Fourier transform infrared (FT-IR) all confirmed the structure of alkyne-terminated poly(methyl methacrylate). The modified surface was characterized by X-ray photoelectron spectroscopy (XPS) after each modification stage. XPS and scanning electron microscope (SEM) were utilized to confirm PMMA-functionalized PI nanofibers, showing polymer coatings present on the surface of PI nanofibers. PI-g-PMMA nanofibers exhibited a more significant reinforcing effect compared to that with ungrafted PI nanofibers.

KEYWORDS: electrospinning • polymer nanofibers • click chemistry • reinforcement

INTRODUCTION

Electrospinning is a highly versatile method for processing solutions or melts, mainly of polymers, into continuous fibers with diameters in the nano- to micrometer range (1, 2). It is predominantly applied to polymer-based materials, including both natural and synthetic polymers; however, in recent years, its application has been extended to metal, ceramic, and glass through the exploitation of precursor routes (3, 4). The nanofibers can be functionalized during electrospinning by introducing porous (5, 6), core−sheath structures (7−11) and by incorporating functional elements such as drugs (12), silver particles (13, 14), carbon nanotubes (15−18), catalysts (19), and even enzymes (20, 21).

The design, fabrication, and characterization of desirable surface properties have attracted much research interest because of their many potential applications, including nanocomposites, microelectronic devices, and biological applications (22). To date, two main strategies, "grafting from" and "grafting to" have been presented and are widely used to modify a solid or polymer surface with polymer chains, giving rise to so-called polymer brushes (23−25). The "grafting from" approach, that is, graft polymerization starting with initiating sites fixed on the surface, promises high graft densities in a good solvent condition, but control over the polymer molecular weight and architecture can be difficult to achieve. Conversely, the "grafting to" approach, which involves polymer preparation prior to grafting, allows full control over the polymer chain length, but typically results in low graft density because of steric hindrance of the grafting of new chains. Nanofibrous morphology is an attractive solution to numerous issues pertaining to the fields of medicine, energy, and the environment. It is important to select suitable materials and appropriate methods in introducing the desired functionality to meet specific needs. Surface-functionalized polymer nanofibers are of growing interest because of their potential applications in various areas. In some early reports, it has been stated that nanofibers can also be functionalized after electrospinning by surface-initiated atom transfer radical polymerization (26), electroless deposition (27, 28), and plasma treatment (29).

Recently, "click" chemistry has attracted significant attention in polymer and materials science. Click chemistry, established by Sharpless and co-workers, is an efficient tool for carrying out polymerizations as well as for modifications of macromolecules and solids (30, 31). In particular, the Cu^1-catalyzed click reaction results in 1,3-dipolar cycloaddition between azides and alkynes even under mild conditions, and the reaction provides products stereoselectively with high yields, produces inoffensive byproduct, and is insensitive to oxygen and water (32, 33). Click chemistry had been used successfully for the preparation of well-defined structural polymer-grafted nanoparticles (34−36), nanofibers (37), carbon nanotubes (38−40), and fullerenes (41). To the best of our knowledge, it has not been used for the surface-modification of high performance nanofibers. Polyimide (PI) is one of the most widely used polymers because of its outing thermal, mechanical, physicochemical, and dielectric properties. The ability to manipulate and enhance the properties of PI is of great importance to its widespread applicable. The use of reinforcing PI nanofibers in polymers to improve their

* To whom correspondence should be addressed. Tel +86-21-67792891. Fax +86-21-67792855. E-mail: cdj@dhu.edu.cn.

Received for review August 18, 2009 and accepted November 27, 2009

DOI: 10.1021/am900553k

Published on Web 12/10/2009

Scheme 1. Preparation of PI-g-PMMA Nanofibers by Click Chemistry

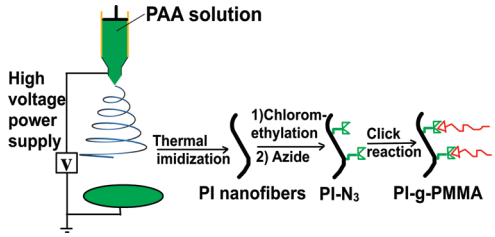

mechanical properties is encountered in polymer technology. It is well-known that there is interphase region between nanofibers and matrix which takes a role to deliver the stress from matrix to reinforcement fibers. Hence, polymer composites with weak interphase generally indicate poor mechanical performance (3). To strengthen the interphase adhesion between nanofibers and matrix, we report a new route to produce functional nanofibers by combining atom-transfer radical polymerization (ATRP) and click coupling to tailor the functionality of PI nanofibers with well-defined poly(methyl methacrylate). A type of polyamic acid (PAA) produced from pyromellitic dianhydride (PMDA) and 4−4′-oxidianiline (ODA) in dimethylacetamide (DMAc) was synthesized by polycondensation. PI nanofibers were prepared via electrospun PAA, followed by thermal imidization. Azide-decorated PI nanofibers were then prepared via chloromethylation, followed by the azide process. The functionalization of PI nanofibers was achieved via click reaction of the azide-decorated PI nanofibers and alkyne-terminated poly(methyl methacrylate) (PMMA), which was prepared by ATRP. The experimental procedures are shown in Scheme 1.

EXPERIMENTAL SECTION

Materials. The solution of oxidianiline-pyromellitic dianhydride PAA in DMAc was provided by our laboratory. The structure of a repeat unit of the PAA is $C_{22}H_{10}N_2O_5$. Propargyl alcohol (99%), *N*,*N*,*N*′,*N*″-pentamethyldiethylenetriamine (PMDETA), 2-bromopropionic acid (99%), *N*,*N*′-dicyclohexylcarbodimide (DCC), and 4-dimethylaminopyridine (DMAP) were purchased from Aldrich Chemical Co. Sodium azide (NaN_3, 99%) and stannic chloride ($SnCl_4$) were purchased from Alfa Aesar and used without further purification. Paraformaldehyde ($(HCOH)_n$, 95%), chlorotrimethylsilane (Me_3SiCl, 97%), methyl methacrylate (MMA, 99%), copper(I) bromide (CuBr, 99%), *N*,*N*-dimethylformamide (DMF), and all other chemicals were purchased from Sinopharm Chemical Reagent Co. Ltd. and used as received.

Sample Synthesis. ***Preparation of Propargyl 2-Bromopropionate.*** The ATRP initiator, propargyl 2-bromopropionate (PBP), was prepared by the esterification of propargyl alcohol with 2-bromopropionic acid in the presence of DCC and DMAP (Scheme 2). A solution of 2-bromopropionic acid (7.65 g, 0.05 mol) and DCC (12.38 g, 0.06 mol) in CH_2Cl_2 (50 mL) was stirred at 0 °C in an ice−water bath, and a solution of propargyl alcohol (2.81 g, 0.05 mol) and DMAP (0.12 g, 0.9 mmol) in methylene chloride (30 mL) was added dropwise over a period of 30 min (33). The reaction mixture was stirred at 0 °C for 1 h and then at room temperature overnight, after which the mixture was filtered and concentrated in a vacuum. The crude product was purified by column chromatography using a gradient eluent of methylene chloride, resulting in an oil liquid with a yield of 80%.

Scheme 2. Synthetic Routes for the Preparation of Well-Defined alkyne-PMMA-Br, via ATRP Reaction

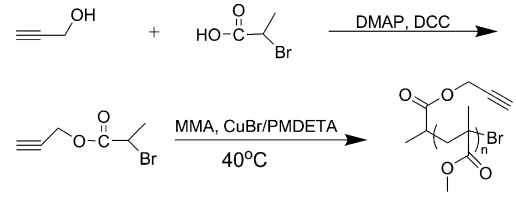

Polymerization of Alkyne−PMMA−Br. A 100 mL round-bottomed flask containing CuBr (0.38 g, 2.65 mmol), PMDETA (0.46 g, 2.65 mmol), MMA (18.89 g, 0.19 mol), and toluene (10 mL) was degassed over three freeze/pump/thaw cycles. After warming to room temperature, 0.39 g (2 mmol) of the initiator (PBP) was added using a syringe. The reaction mixture was placed in a water bath preheated at 40 °C and allowed to stir under a nitrogen atmosphere for 4 h (Scheme 2). The reaction mixture was then cooled to room temperature and dissolved in tetrahydrofuran (THF) before being passed through a neutral alumina column into methanol to remove copper catalysts. The obtained product as a white solid was dried in a vacuum oven for 24 h (yield of 45%; M_n = 9500 from gel permeation chromatography (GPC); M_w/M_n = 1.26).

Fabrication of PI Nanofibers. A typical electrospinning setup was used for the experiments. The synthesized PAA solution was electrospun into nanofibers onto aluminum foil. Electrospinning was carried out using a syringe and a high voltage from a DC power supply of 30 kV over a 15 cm gap between the spinneret and collector. A microinfusion pump was set to deliver the solution at a flow rate of 10 mL/h using a 1 mL syringe. All experiments were conducted at room temperature with 60% humidity. The PAA nanofiber mat that was removed from the substrate was then converted into a PI nanofiber mat via thermal imidization in a high-temperature furnace. The procedure, which has several different oxidation steps, is described elsewhere (42).

Chloromethylation of the PI Nanofiber Surfaces. The chloromethylation of PI was conducted according to previously reported procedures (43, 44). For the typical chloromethylation reaction, 30 mL of chloroform, 1.5 g of $(HCOH)_n$, 6.5 mL of Me_3SiCl, and 3 mL of $SnCl_4$ were introduced into a round-bottom flask that contained the PI nanofibers. The reaction mixture was kept at 50 °C for 6 h to produce the chloromethylated PI nanofibers (PI−Cl). The introduced chloromethyl groups yield azide-decorated PI nanofibers for the click reaction. After the reaction, the PI−Cl surface was washed exhaustively with excess amounts of acetone and water.

Synthesis of Azide-Decorated PI Nanofibers. The chloro-decorated polyimide (PI−Cl) nanofibers were reacted with an excess of NaN_3 at room temperature in DMF (50 mL) to yield azide-decorated polymers (PI−N_3). PI−N_3 was thus obtained after washing and then drying overnight in a vacuum oven.

Click coupling of PI−N_3 and Alkyne−PMMA−Br. PI−N_3 was suspended in 30 mL of DMF in a 50 mL round-bottomed flask. The solution was deoxygenated by bubbling with nitrogen for at least 30 min. An excess amount of alkyne−PMMA−Br was added along with CuBr (0.23 g, 1.6 mmol) and PMDETA (0.27 g, 1.6 mmol) under the protection of N_2 flow. The reaction was allowed to proceed at room temperature for 24 h. PI-g-PMMA nanofibers were removed from the mixture and then washed with DMF and water three times to remove noncovalently bound alkyne−PMMA−Br. After purification, the resulting products were dried overnight in a vacuum oven, resulting in PMMA-grafted PI nanofibers.

Characterization. The molecular weight and polydispersity of polymers were determined by GPC (BI-MWA, Waters, USA). A solution was made by dissolving the samples in HPLC-grade tetrathydrofuran (THF); this solution was then filtered twice

Table 1. Grafting Yield of the Surface-Modified PI Nanofibers with Well-Defined Poly(methyl methacrylate)

	alkyne-terminated poly(methyl methacrylate) precursors[a]				
sample	reaction time (h)	M_n (g/mol)[b]	PDI[b]	click reaction time (h)[c]	grafting yield (%)[d]
PI-g-PMMA1	4	9500	1.26	24	16.5
PI-g-PMMA2	6	12300	1.18	24	18.3
PI-g-PMMA3	8	13500	1.21	24	20.4

[a] Atom transfer radical polymerization (ATRP) of methyl methacrylate in Table 1 were carried out at 40 °C in toluene containing CuBr (0.38 g, 2.65 mmol), PMDETA (0.46 g, 2.65 mmol), MMA (18.89 g, 0.19 mol), and the initiator PBP (0.39 g, 2 mmol). [b] Obtained from GPC analysis using THF as eluent. [c] The "click" reaction between azide-decorated polyimide nanofibers and excess amount of alkyne-terminated poly(methyl methacrylate) was carried out under the catalysis of Cu(I)Br/ N,N,N′,N″-pentamethyldiethylenetriamine (PMDETA). [d] Grafting yield is defined as $(W_a - W_b)/W_b$, where W_a and W_b represent the weight of the dry nanofibers after and before grafting, respectively.

through 0.2 μm filters. ^{1}H NMR spectra were recorded in $CDCl_3$ using a Bruker AVANCE-300 spectrometer. Fourier transform infrared spectra (FT-IR) were recorded on a Nicolet NEXUS-670 spectrometer with KBr pellets. The morphology of the functional nanofibers, which were gold-sputtered prior to observation, was observed with a JSM-5600LV scanning electron microscope at an accelerating voltage of 10 kV. Pristine and modified PI nanofiber surfaces were analyzed by X-ray photoelectron spectroscopy (XPS) using a Kratos AXIS HIS spectrometer and a monochromatized Al Kα X-ray source (1486.6 eV photons). The pressure in the analysis chamber was maintained at 1×10^{-6} Pa or less during each measurement. Surface elemental stoichiometries were determined from the sensitivity-factor-corrected spectral area ratios and were reliable within ±10%. Tensile tests were carried out on a Universal material testing machine (DXL-2000). Fiber diameters were calculated on the basis of the SEM micrographs using graphic measurement software and 50 fibers for each sample were randomly measured. The humidity of the laboratory was about 60%.

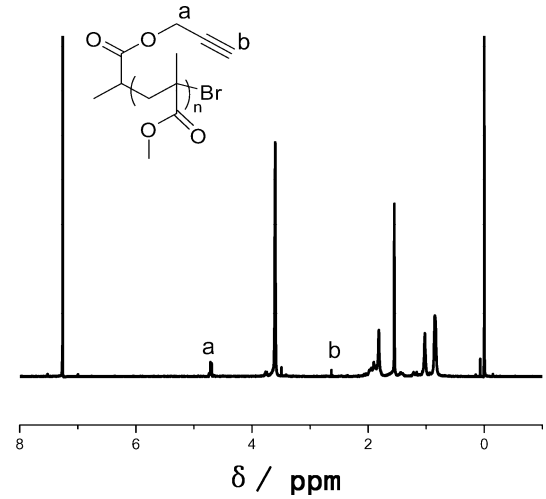

FIGURE 1. ^{1}H NMR spectrum of alkyne−PMMA−Br in $CDCl_3$.

RESULTS AND DISCUSSION

In general, three processes are needed in sequence for the preparation of PMMA-grafted PI nanofibers: alkyne−PMMA−Br preparation, azide-decorated PI nanofibers preparation, and click coupling. The route would involve the former reaction of chloromethylation and azide process for PI nanofibers and subsequent click reaction of azide-decorated PI nanofibers and alkyne−PMMA−Br. There are two main synthetic routes to polyimide, namely two-step and one-step processing (45). Because ODA-PMDA PI is insoluble in all organic and inorganic solvents except for sulfuric acid, the two step processing was used to produce PI nanofibers. The pristine PAA (precursor of PI) nanofibers prepared by electrospinning are imidized in a high-temperature furnace to form PI nanofibers, which have a larger surface area to volume ratio than that of fibers prepared from conventional fiber spinning techniques, thereby enabling the realization of applications requiring finer structures.

Atom transfer radical polymerization (ATRP) has been shown to be a versatile technique for the controlled polymerization of many monomers. The fundamental principle underlying ATRP is halogen exchange during polymerization between the halogen-terminated growing polymer chain/Cu(I) complex and macroradical/Cu(II) complex. The bromoesters are known to be effective initiators for the ATRP of styrene, acrylic, methylmethacrylate, and other vinyl monomers (46). PBP has been successfully used as the initiator for the preparation the polystyrene with alkyne-terminated groups by Masuda et al. (47). In the current study, similar protocols were employed for the ATRP of MMA monomer. Scheme 2 illustrates the process used to synthesize the initiator with alkyne groups. PBP was prepared via the reaction between the hydroxyl groups of propargyl alcohol and the carboxylic acid groups of 2-bromopropionic acid in the presence of both DCC and DMAP. The reaction produced an alkyne-terminated initiator. To study the influence of different molecular weights on the thickness of the grafting layer, we prepared a series of well-defined PMMA polymers via ATRP using PBP as an initiator and a CuBr/PMDETA complex as the catalyst. The polymerization proceeded under good control, as confirmed by the low product polydispersity. Good control over molecular weights and low polydispersities were observed (Table 1). Alkyne terminal groups were attached to the polymers after polymerization of MMA was finished. The chemical structure of alkyne-PMMA-Br was confirmed by both ^{1}H NMR and FT-IR. In the ^{1}H NMR spectrum of alkyne-PMMA-Br (Figure 1), peak a (4.7 ppm) can be ascribed to methylene protons (2H) of propargyl residues. Peak b (2.6 ppm) can be ascribed to an alkyne proton. Moreover, the FT-IR spectrum of alkyne-PMMA-Br clearly revealed the appearance of an absorbance peak at 3300.8 cm^{-1}, which is characteristic of the CH stretching vibrations of the terminal alkyne groups (Figure 2). The peak at 2130.0 cm^{-1} is attributed to C≡C stretching vibrations because of the immobilization of C≡C bonds in the polymer chains.

In the preparation of PI-g-PMMA via click coupling, azide groups on the PI nanofiber surfaces are indispensable. In this

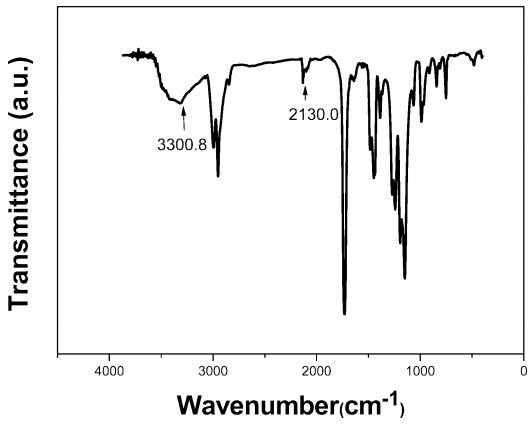

FIGURE 2. FT-IR spectrum obtained for alkyne−PMMA−Br.

Scheme 3. Synthetic Routes for the Preparation of PI-g-PMMA, via Click Coupling

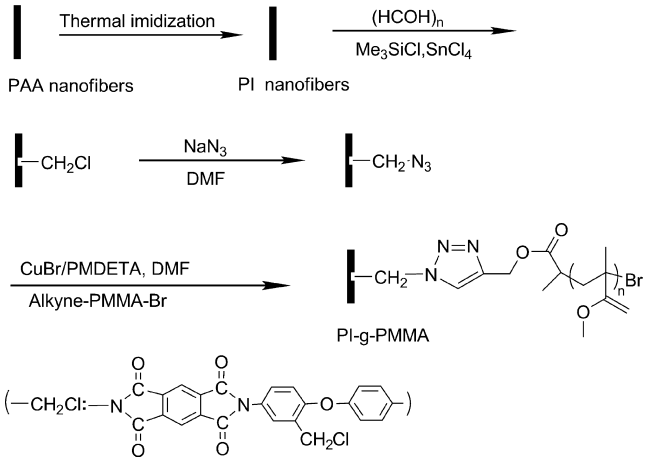

work, a two-step process was developed for the immobilization of azide groups on the nanofiber surfaces (Scheme 3): (1) PI nanofibers were chloromethylated in a simple one-step process to introduce the chloromethyl groups and (2) the chloromethyl groups of the PI−Cl nanofiber were reacted with NaN_3 to produce azide-decorated PI nanofibers.

The pristine and modified PI nanofibers were characterized by XPS (43, 44). Figure 3 shows the XPS wide scan and C 1s core-level spectra of pristine PI and the PI−Cl surfaces, and reveals a Cl 2p signal at a binding energy (BE) of about 199.3 eV. The corresponding Cl 2p core-level spectrum consisted of Cl $2p_{3/2}$ and Cl $2p_{1/2}$ peak components at BEs of about 199.3 and 200.7 eV, respectively (Figure 4), which is characteristic of covalently bonded chlorine. The C 1s core-level spectra of the PI and PI−Cl surfaces can be curve-fitted into four peak components with BEs of about 284.7, 285.2, 286.4, and 288.7 eV, attributable to the C−H, C−N, C−O (and C−Cl for the PI−Cl surface), and $N(C{=}O)_2$ species, respectively (48, 49). The $\pi-\pi^*$ shakeup satellite was also discernible at a BE of about 291.5 eV for the aromatic rings at the PI surface. The peak of the $\pi-\pi^*$ shakeup satellite weakens after the chloromethylation of the PI nanofibers, which is consistent with previously reported results (43). The [Cl]/[C] ratio was about 0.04, which was determined from sensitivity-factor-corrected Cl 2p and C 1s core-level spectral area ratio. This indicates that active chloromethyl groups were introduced onto the PI nanofiber surface. PI−Cl can provide effective macroinitiators for the surface initiated ATRP (43). Here, it should be noted that PI nanofibers with chloromethyl groups can become involved in a nucleophilic substitution reaction with NaN_3.

A control experiment in which PI−Cl was reacted with excess NaN_3 under gentle reaction conditions was carried out to achieve more complete surface coverage of the functional nanofibers (Scheme 3). After the conversion of chlorine into azide, the Cl 2p peak disappeared completely on the surface of PI nanofibers, as shown in Figure 5, indicating the complete conversion of chlorine to azide functional groups. Figure 6b shows the results of the XPS study carried out on N 1s data obtained for an azide-decorated surface. Peaks appear at 399.8 and 403.6 eV, as expected for azide groups on the surface, in the region that showed only a single peak for the PI−Cl precursor (Figure 6a). The peak splitting indicates the presence of two nitrogen species at the azide-decorated PI surface, which reflects the differently charged nitrogen atoms in the azide groups (50). Moreover, the FT-IR spectrum of PI−N_3 clearly revealed the appearance of an absorbance peak at 2107 cm^{-1}, which is characteristic of the azide groups (Figure 7a).

Such functionalized azide-decorated PI nanofibers provide a substrate that could be employed in 1,3-dipolar cycloaddition reactions if reacted with terminal alkyne-substituted polymer chains. The Huisgen 1,3-dipolar cycloaddition between azides and alkynes is facilitated by the presence of Cu(I) ions. The advantage of the copper catalysis is not only lowering the required reaction temperature but also having higher regionspecificity of the reaction leading only to 1,4-triazoles (51). For preparation of PI-g-PMMA nanofibers, click coupling was carried out in a round-bottom flask. The azide-terminated PI nanofibers were placed in the flask containing a solution of alkyne−PMMA−Br, CuBr, and PMDETA in DMF solvent. The reaction was allowed to proceed at room temperature for 24 h under a continuous supply of nitrogen. The excess alkyne−PMMA−Br and residual catalyst were removed by washing the substrate with a sequence of different solvents. XPS investigations were performed to understand the chemical transformation of the substrates of PI−N_3 after click coupling with alkyne-PMMA-Br. Figure 8a shows the wide-scan and C 1s core-level spectrum of the PI-g-PMMA surface. The wide-scan spectrum detected Br 3d (at a BE of about 71 eV) and Br 3p (at a BE of about 184 eV) signals, characteristic of covalently bonded bromine (48), which are attributable to click coupling between PI−N_3 and alkyne-PMMA-Br. In Figure 8b, the C 1s core-level spectrum of the PI-g-PMMA surface is fitted to three peak components with BEs of about 284.9, 286.3, and 288.9 eV, which are attributable to the C−H, C−O/C−Br, and C═O species, respectively, and suggest that the surface of PI-g-PMMA nanofibers are covered by the PMMA (52). The XPS N 1s results in Figure 8c reveal additional evidence of 1,2,3-triazole formation on PI surface; only a single peak is evident at 399.8 eV, thus confirming the reaction between azide and alkyne groups. Moreover, we can observe the

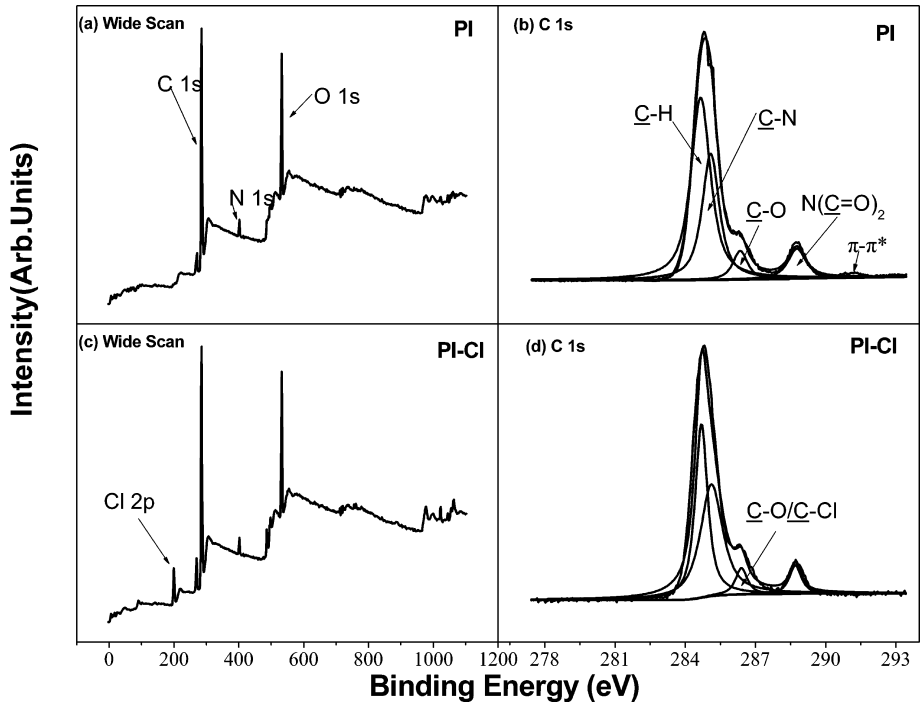

FIGURE 3. X-ray photoelectron spectroscopy (XPS) wide-scan and C 1s core-level spectra of the (a, b) pristine PI nanofiber surface, (c, d) PI−Cl surface.

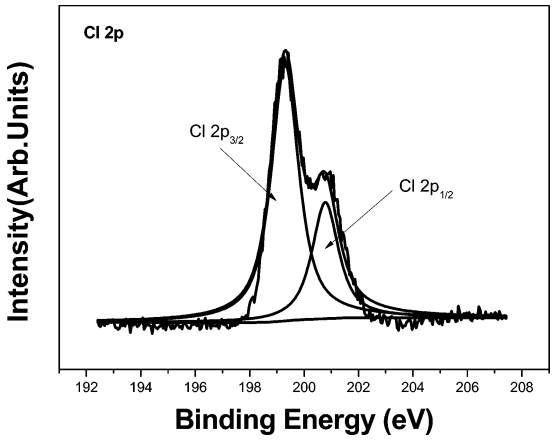

FIGURE 4. Cl 2p core-level spectrum of PI−Cl surface.

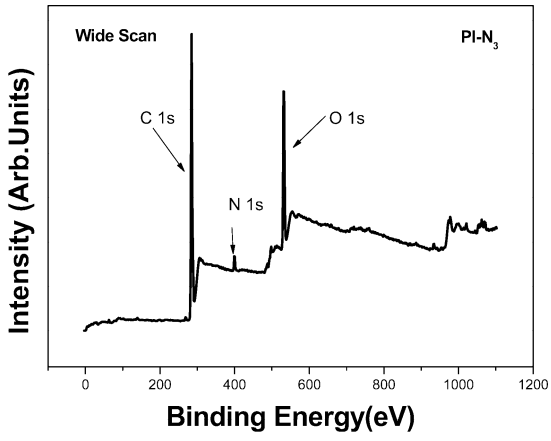

FIGURE 5. Wide-scan spectrum of the PI−N_3 surface.

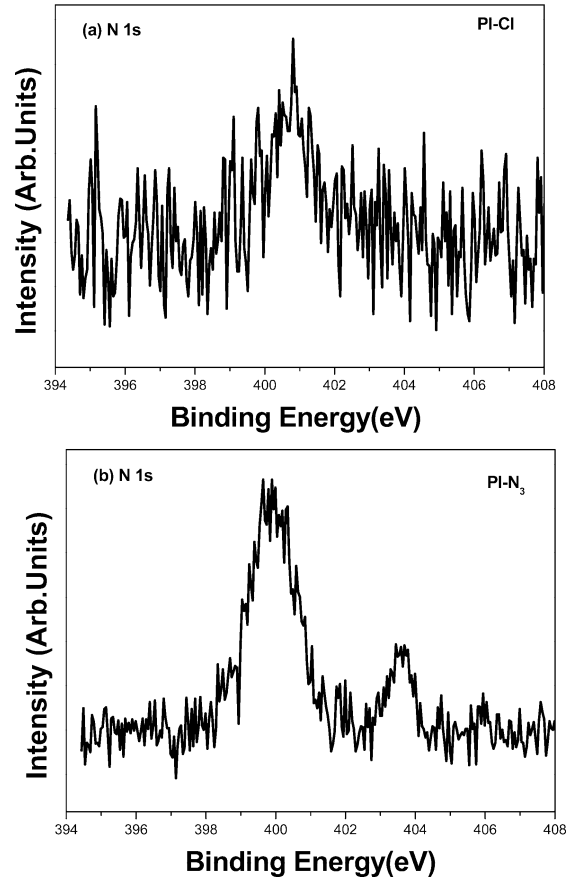

FIGURE 6. XPS spectra of the N 1s region of (a) chlorine-, (b) azide-decorated PI nanofibers.

complete disappearance of characteristic azide absorbance peak at 2107 cm^{-1} for PI-g-PMMA nanofibers, confirming that the azide groups were all consumed in the click reaction (Figure 7b). Grafting yield was defined as $W_a - W_b/W_b$, where W_a and W_b were the weight of the dry nanofibers after and before grafting the nanofibers. These values for PI-g-

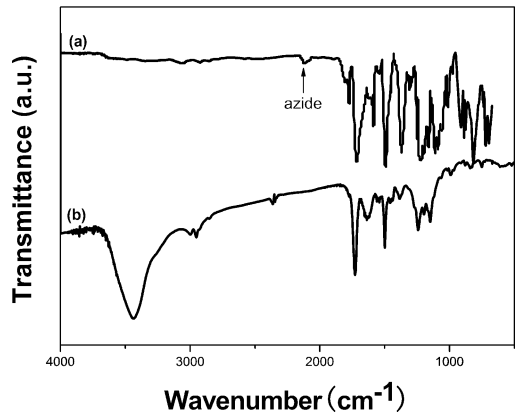

FIGURE 7. FT-IR spectra obtained for (a) PI−N_3 and (b) PI-g-PMMA nanofibers.

PMMA1, PI-g-PMMA2, and PI-g-PMMA3 are about 16.5, 18.3, and 20.4%, respectively. The enhanced grafting yield after click reaction is associated with a corresponding increase in molecular weight of alkyne-terminated PMMA (Table 1).

A microstructural examination was carried out by SEM to evaluate the effect of the surface modification of PI nanofibers by click chemistry (Figure 9). The images showed that pristine PI nanofibers with a diameter of ~230 ± 4 nm (Figure 9a) were much smoother than PI-g-PMMA (Figure 9b). After surface modification with PMMA, SEM confirmed (1) the presence of a rough surface morphology with many small grainy deposits on the surfaces of PI nanofibers and (2) an increase in the average diameter of the nanofibers, the diameters for PI-g-PMMA1, PI-g-PMMA2, and PI-g-PMMA3 surfaces have increased to ~240 ± 3, ~250 ± 5, and ~255 ± 6 nm, indicating that the present reaction immobilizes a dense layer of PMMA. The alignment of nanofibers along a certain direction is of interest for nanofiber reinforcement or for tissue engineering in order to distribute these reinforcing nanofibers or allow a distinct growth direction for the cell and for many more applications (2). Here, the PAA nanofibers were collected using two conductive sheets, according to Xia's report (53). A collector was fabricated by placing two copper sheets within a distance of 40 mm. The PAA nanofibers were stretched across the gap between the two sheets to form a parallel array. Uniaxially aligned arrays of PI-g-PMMA nanofibers were prepared after the previous procedures. Figure 10 shows an image of the PI-g-PMMA arrays. The distance between parallel electrodes is 40 mm; therefore, the PI-g-PMMA nanofibers with uniaxial alignment are about 40 mm. The image shows uniaxially aligned PI-g-PMMA nanofibers with rough surface morphology. A few PI-g-PMMA nanofibers are not parallel with the most of nanofibers but cross the aligned nanofibers.

It is often mentioned that electrospun fibers can be used as a reinforcement component in composites, but the number of investigations on this topic is rather small. The main problems, to which there are no convincing solutions yet, are the control of the nanofiber alignment in the polymer matrix and the enforcing interface compatibility between nanofiber and the polymer matrix (3). In the

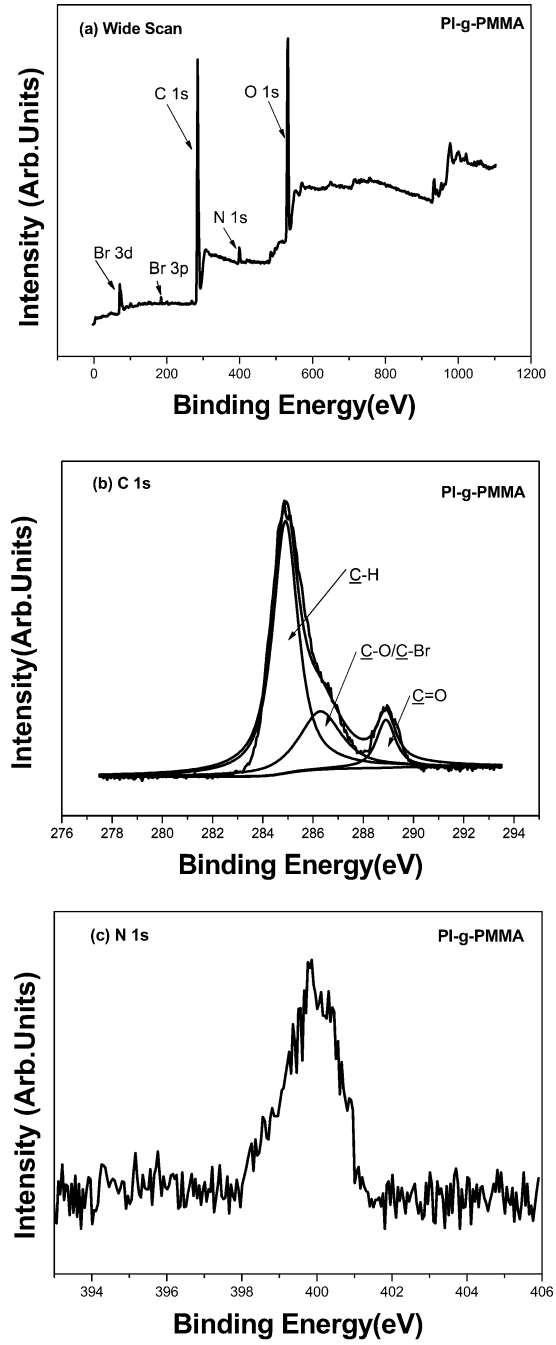

FIGURE 8. (a) Wide-scan and (b) C 1s core-level spectra of the PI-g-PMMA surface, and (c) N 1s spectrum of PI-g-PMMA surface.

previous reports, pure random electrospun nanofibers tended to display enhanced mechanical properties in polymer matrix (54, 55). Here, the PI-g-PMMA nanofibers with aligned arrays can be used as reinforcing fillers in PMMA matrix. To compare the influence of the modification on the mechanical properties of the composites, we respectively immersed the PI and PI-g-PMMA nanofibers in a mixture of MMA monomer, 2, 2′-azobisisobutyronitrile (AIBN) as the initiator; we then carried out in situ polymerization at 60 °C for 16 h. SEM was used to check the morphologies of the PI-g-PMMA in polymer matrix. To observe the morphology of the nanofibers in PMMA matrix, we stuck the nanofibers to bottom of the glass mold. Most of nanofibers were embed-

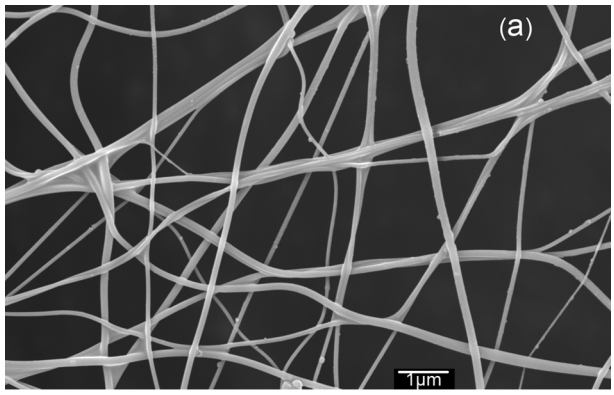

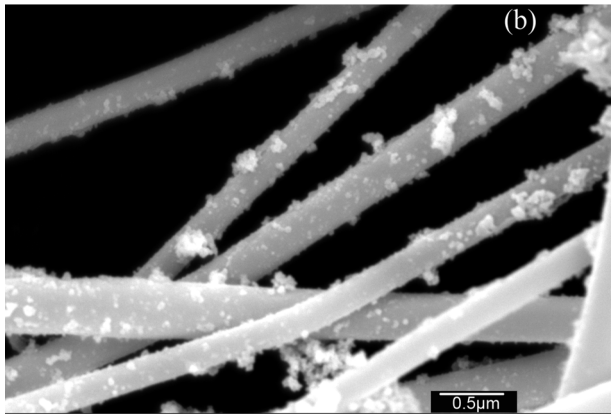

FIGURE 9. SEM images of (a) pristine PI nanofibers and (b) PI-g-PMMA nanofibers.

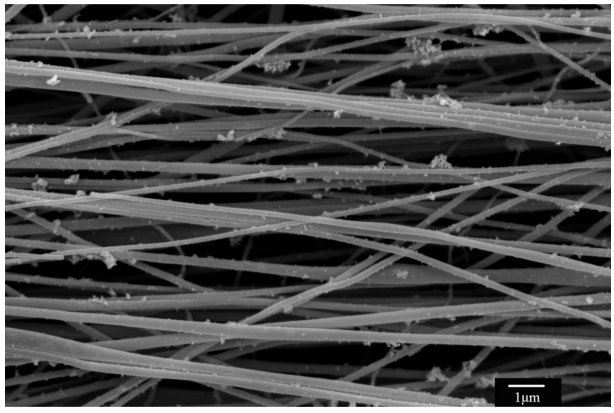

FIGURE 10. SEM image of the uniaxially aligned PI-g-PMMA nanofibers.

ded in matrix after in situ polymerization. A part of nanofibers embedded in polymer matrix from the bottom of the glass mold was exposured. Figures 11 and 12 give images with different magnifications of the uniaxially aligned PI-g-PMMA nanofibers in PMMA matrix. As shown in Figure 12, the image shows a fuzzy interphase between PI-g-PMMA nanofibers and PMMA matrix. The tensile strength, the tensile modulus, and the elongation at break of composites are summarized in Table 2 (nanofiber axial direction). In contrast with PI/PMMA composite, it was found that tensile modulus was not affected by the addition of modified nanofibers. However, the addition of three kind of PI-g-PMMA (10 wt %, respectively) leads to the significant increase of tensile strength by ~36, ~38, and ~40%,

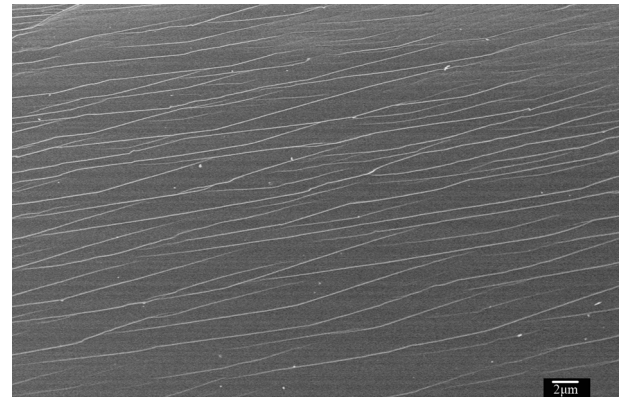

FIGURE 11. SEM image with low magnification of the PMMA matrix with the uniaxially aligned PI-g-PMMA nanofibers.

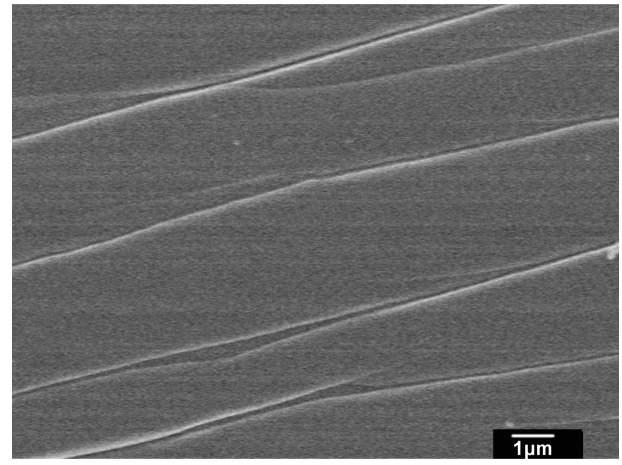

FIGURE 12. SEM image with high magnification of the PMMA matrix with the uniaxially aligned PI-g-PMMA nanofibers.

Table 2. Tensile Properties of PMMA and PMMA Composites with Different Uniaxially Aligned PI Nanofibers

sample[a]	tensile strength (MPa)	tensile modulus (GPa)	elongation at break (%)
Pure PMMA	26.04	1.40	1.29
PI/PMMA	40.61	3.61	1.04
PI-g-PMMA1/PMMA	55.35	3.62	1.32
PI-g-PMMA2/PMMA	56.13	3.58	1.45
PI-g-PMMA3/PMMA	56.71	3.51	1.57

[a] In this case, all of the polymers were prepared by in situ polymerization, which was carried out at 60 °C for 16 h. The all loadings of PI and PI-g-PMMA in PMMA matrix are 10 wt %.

verifying the validity of enforcing interfaces compatibility by grafting PMMA to PI surface. In addition, PI-g-PMMA nanofibers are likely to participate in bulk polymerization. The grafting PMMA-Br of PI-g-PMMA nanofibers may be converted to living free radical for chain growth polymerization or inhibiting polymer chains in bulk polymerization (56). This method is expected to achieve large interfacial shear strength because of the strong, even covalent interaction. However, it should be pointed out that the tensile strength did not significantly increase with the increase in molecular weight of grafted PMMA, which indicated that the increase in molecular weight did not enhance interfacial shear strength further.

CONCLUSION

This study proposes a facile method for surface modification of PI nanofibers with well-defined PMMA by combining electrospinning and click chemistry. This new approach represents a rapid, convenient, and versatile synthesis of modified PI nanofibers with PMMA using mild conditions associated with click chemistry. The polymer grafting was confirmed by XPS and SEM analyses. Because of the applicability of ATPR to a wide variety of functional monomers, surface functionalization of PI nanofibers with various linear chains can be readily prepared. This kind of modification technique can significantly enforce interface compatibility with the host matrix when PI-g-PMMA nanofibers as reinforcing fillers have been incorporated into the PMMA matrix. In addition, a dense packing of nanofibers with functional polymers is highly desirable, especially for medical applications and device development. With the selection of appropriate nanofibers and use of tailor-made surface functionalities, click chemistry can provide a powerful tool for the functionalization of nanofibers.

Acknowledgment. This work has been supported by the Fund of Innovation Project on Doctoral Dissertation of Donghua University and Supported by the Programme of Introducing Talents of Discipline to Universities (111-2-04).

REFERENCES AND NOTES

(1) Dzenis, Y. *Science* **2004**, *304* (5679), 1917–1919.
(2) Teo, W. E.; Ramakrishna, S. *Nanotechnology* **2006**, *17* (14), R89–R106.
(3) Greiner, A.; Wendorff, J. H. *Angew. Chem., Int. Ed.* **2007**, *46* (30), 5670–5703.
(4) Reneker, D. H.; Yarin, A. L.; Zussman, E.; Xu, H. *Adv. Appl. Mech.* **2007**, *41*, 43–195.
(5) Bognitzki, M.; Czado, W.; Frese, T.; Schaper, A.; Hellwig, M.; Steinhart, M.; Greiner, A.; Wendorff, J. H. *Adv. Mater.* **2001**, *13* (1), 70–72.
(6) Megelski, S.; Stephens, J. S.; Chase, D. B.; Rabolt, J. F. *Macromolecules* **2002**, *35* (22), 8456–8466.
(7) Wei, M.; Lee, J.; Kang, B. W.; Mead, J. *Macromol. Rapid Commun.* **2005**, *26* (14), 1127–1132.
(8) McCann, J. T.; Li, D.; Xia, Y. N. *J. Mater. Chem.* **2005**, *15* (7), 735–738.
(9) Ojha, S. S.; Stevens, D. R.; Stano, K.; Hoffman, T.; Clarke, L. I.; Gorga, R. E. *Macromolecules* **2008**, *41* (7), 2509–2513.
(10) Xu, X. L.; Zhuang, X. L.; Chen, X. S.; Wang, X. R.; Yang, L. X.; Jing, X. B. *Macromol. Rapid Commun.* **2006**, *27* (19), 1637–1642.
(11) Xin, Y.; Huang, Z. H.; Li, W. W.; Jiang, Z. J.; Tong, Y. B.; Wang, C. *Eur. Polym. J.* **2008**, *44* (4), 1040–1045.
(12) Verreck, G.; Chun, I.; Rosenblatt, J.; Peeters, J.; Van Dijck, A.; Mensch, J.; Noppe, M.; Brewster, M. E. *J. Controlled Release* **2003**, *92* (3), 349–360.
(13) Wang, Y. Z.; Li, Y. X.; Sun, G.; Zhang, G. L.; Liu, H.; Du, J. S.; Yang, S. A.; Bai, J.; Yang, Q. B. *J. Appl. Polym. Sci.* **2007**, *105* (6), 3618–3622.
(14) Lee, H. K.; Jeong, E. H.; Baek, C. K.; Youk, J. H. *Mater. Lett.* **2005**, *59* (23), 2977–2980.
(15) Sen, R.; Zhao, B.; Perea, D.; Itkis, M. E.; Hu, H.; Love, J.; Bekyarova, E.; Haddon, R. C. *Nano Lett.* **2004**, *4* (3), 459–464.
(16) Hou, H. Q.; Ge, J. J.; Zeng, J.; Li, Q.; Reneker, D. H.; Greiner, A.; Cheng, S. Z. D. *Chem. Mater.* **2005**, *17* (5), 967–973.
(17) Kannan, P.; Eichhorn, S. J.; Young, R. J. *Nanotechnology* **2007**, *18* (23), 235707/1–235707/7.
(18) Zhang, Q. H.; Chang, Z. J.; Zhu, M. F.; Mo, X. M.; Chen, D. J. *Nanotechnology* **2007**, *18* (11), 115611/1–115611/6.
(19) Im, J. S.; Kim, M. I.; Lee, Y. S. *Mater. Lett.* **2008**, *62* (21–22), 3652–3655.
(20) Herricks, T. E.; Kim, S. H.; Kim, J.; Li, D.; Kwak, J. H.; Grate, J. W.; Xia, Y. N. *J. Mater. Chem.* **2005**, *15* (31), 3241–3245.
(21) Jia, H. F.; Zhu, G. Y.; Vugrinovich, B.; Kataphinan, W.; Reneker, D. H.; Wang, P. *Biotechnol. Prog.* **2002**, *18* (5), 1027–1032.
(22) Ruckenstein, E.; Li, Z. F. *Adv. Colloid Interface Sci.* **2005**, *113* (1), 43–63.
(23) Edmondson, S.; Vo, C. D.; Armes, S. P.; Unali, G. F.; Weir, M. P. *Langmuir* **2008**, *24* (14), 7208–7215.
(24) Liu, Y. L.; Chen, W. H. *Macromolecules* **2007**, *40* (25), 8881–8886.
(25) Nagase, K.; Kobayashi, J.; Kikuchi, A. I.; Akiyama, Y.; Kanazawa, H.; Okano, T. *Langmuir* **2008**, *24* (2), 511–517.
(26) Fu, G. D.; Lei, J. Y.; Yao, C.; Li, X. S.; Yao, F.; Nie, S. Z.; Kang, E. T.; Neoh, K. G. *Macromolecules* **2008**, *41* (18), 6854–6858.
(27) Pinto, N. J.; Carrion, P.; Quinones, J. X. *Mater. Sci. Eng., A* **2004**, *366* (1), 1–5.
(28) Tao, D.; Wei, Q. F.; Cai, Y. B.; Xu, Q. X.; Sun, L. Y. *J. Coat. Technol. Res.* **2008**, *5* (3), 399–403.
(29) Duan, Y.; Wang, Z.; Yan, W.; Wang, S.; Zhang, S.; Jia, J. *J. Biomater. Sci., Polym. Ed.* **2007**, *18*, 1153–1164.
(30) Kolb, H. C.; Finn, M. G.; Sharpless, K. B. *Angew. Chem., Int. Ed.* **2001**, *40* (11), 2004–2021.
(31) Wu, P.; Feldman, A. K.; Nugent, A. K.; Hawker, C. J.; Scheel, A.; Voit, B.; Pyun, J.; Frechet, J. M. J.; Sharpless, K. B.; Fokin, V. V. *Angew. Chem., Int. Ed.* **2004**, *43* (30), 3928–3932.
(32) Binder, W. H.; Sachsenhofer, R. *Macromol. Rapid Commun.* **2007**, *28* (1), 15–54.
(33) Xu, J.; Ye, J.; Liu, S. Y. *Macromolecules* **2007**, *40* (25), 9103–9110.
(34) O'Reilly, R. K.; Joralemon, M. J.; Wooley, K. L.; Hawker, C. J. *Chem. Mater.* **2005**, *17* (24), 5976–5988.
(35) Fischler, M.; Sologubenko, A.; Mayer, J.; Clever, G.; Burley, G.; Gierlich, J.; Carell, T.; Simon, U. *Chem. Commun.* **2008**, 169–171.
(36) He, H.; Zhang, Y.; Gao, C.; Wu, J. Y. *Chem. Commun.* **2009**, 1655–1657.
(37) Fu, G. D.; Xu, L. Q.; Yao, F.; Zhang, K.; Wang, X. F.; Zhu, M. F.; Nie, S. Z. *ACS Appl. Mater. Interfaces* **2009**, *1* (2), 239–243.
(38) Li, H. M.; Cheng, F. O.; Duft, A. M.; Adronov, A. *J. Am. Chem. Soc.* **2005**, *127* (41), 14518–14524.
(39) Zhang, Y.; He, H. K.; Gao, C. *Macromolecules* **2008**, *41* (24), 9581–9594.
(40) Zhang, Y.; He, H.; Gao, C.; Wu, J. Y. *Langmuir* **2009**, *25* (10), 5814–5824.
(41) Zhang, W. B.; Tu, Y.; Ranjan, R.; Van Horn, R. M.; Leng, S.; Wang, J.; Polce, M. J.; Wesdemiotis, C.; Quirk, R. P.; Newkome, G. R.; Cheng, S. Z. D. *Macromolecules* **2008**, *41* (3), 515–517.
(42) Huang, C. B.; Chen, S. L.; Reneker, D. H.; Lai, C. L.; Hou, H. Q. *Adv. Mater.* **2006**, *18* (5), 668–671.
(43) Xu, F. J.; Zhao, J. P.; Kang, E. T.; Neoh, K. G. *Ind. Eng. Chem. Res.* **2007**, *46* (14), 4866–4873.
(44) Li, L.; Ke, Z. J.; Yan, G. P.; Wu, J. Y. *Polym. Int.* **2008**, *57* (11), 1275–1280.
(45) Zhang, Q. H.; Dai, M.; Ding, M. X.; Chen, D.; Gao, L. X. *Eur. Polym. J.* **2004**, *40* (11), 2487–2493.
(46) Matyjaszewski, K.; Xia, J. H. *Chem. Rev.* **2001**, *101* (9), 2921–2990.
(47) Zhang, W.; Shiotsuki, M.; Masuda, T. *Macromol. Chem. Phys.* **2006**, *207* (11), 933–940.
(48) Moulder, J. F.; Stickle, W. F.; Sobol, P. E.; Bomben, K. D., In *X-ray Photoelectron Spectroscopy*; Perkin-Elmer: Eden Prairie, MN, 1992; pp 40,41,44,47,61,62,92.
(49) Inagaki, N.; Tasaka, S.; Hibi, K. *J. Polym. Sci., Part A: Polym. Chem.* **1992**, *30*, 1425–1431.
(50) Devadoss, A.; Chidsey, C. E. D. *J. Am. Chem. Soc.* **2007**, *129* (17), 5370–5371.
(51) Quemener, D.; Le Hellaye, M.; Bissett, C.; Davis, T. P.; Barner-Kowollik, C.; Stenzel, M. H. *J. Polym. Sci., Part A: Polym. Chem.* **2008**, *46* (1), 155–173.
(52) Liu, P.; Su, Z. X. *Polym. Int.* **2005**, *54* (11), 1508–1511.
(53) Li, D.; Wang, Y. L.; Xia, Y. N. *Nano Lett.* **2003**, *3* (8), 1167–1171.
(54) Kim, J. S.; Reneker, D. H. *Polym. Compos.* **1999**, *20* (1), 124–131.
(55) Bergshoef, M. M.; Vancso, G. J. *Adv. Mater.* **1999**, *11* (16), 1362–1365.
(56) Braunecker, W. A.; Matyjaszewski, K. *Prog. Polym. Sci.* **2007**, *32* (1), 93–146.

AM900553K